

RESEARCH ARTICLE

Open Access



Damage model for simulating cohesive fracture behavior of multi-phase composite materials

Mao Kurumatani*, Takumi Kato and Hiromu Sasaki

*Correspondence:
mao.kurumatani.jp@vc.ibaraki.ac.jp

Department of Civil,
Architectural, and Environmental
Engineering, Ibaraki University,
Hitachi, Japan

Abstract

We propose a new damage model for simulating the cohesive fracture behavior of multi-phase composite materials such as concrete. The proposed model can evaluate the damage of the matrix-phase in composite materials using the volume fraction of the matrix within an element comprising the matrix and other materials. The damage model was first formulated for 1D problems and then extended to two-dimensional (2D) and three-dimensional (3D) problems using the equivalent strain based on the modified von-Mises criterion. The validity of the damage model was verified for 1D and 2D problems, and the model was also applied to the simulation of 3D cohesive crack growth in a heterogeneous solid with a large number of spherical inclusions. The results confirm that the proposed model allows the meshless finite element analysis of cohesive fracturing in composite materials.

Keywords: Damage model, Multi-phase composite, Cohesive fracture, Concrete, Meshless analysis

Introduction

Concrete is widely used as a construction material in civil engineering structures, and can be considered as a heterogeneous material comprising a mortar matrix and coarse-aggregate inclusions in the meso-scale, which corresponds to centimeter scale. Generally, mortar without aggregates and concrete with aggregates exhibit different fracture behaviors, and therefore have different material strength and toughness. Concrete has higher toughness than mortar owing to the presence of coarse aggregates, which complicates the concrete's fracture behavior and results in cracks generating and propagating dispersedly at various locations within the concrete. This implies that coarse aggregates play a mechanically significant role in the deformation and fracture behavior of concrete.

In ordinary concrete, cracks rarely penetrate coarse aggregates. In many cases, cracks propagate within the mortar and around the coarse aggregates. To reproduce this fracture behavior using numerical analysis, it is necessary to prepare an analysis mesh that reflects the geometry and distribution of aggregates, and to simulate the cohesive crack propagation behavior of mortar. However, such an analysis mesh for a heterogeneous structure with plenty of aggregates is difficult to generate owing to the aggregates' various shapes

and random distribution. Moreover, even if the mesh could be prepared, it would still be difficult to simulate the cohesive crack propagation behavior. The mesh generation for a complicated micro- or meso-structure, and the analysis of crack propagation are both major challenges for computational mechanics and the finite element method (FEM).

Numerical analyses for the crack propagation behavior in the concrete's meso-scale have been conducted, and many such analyses have employed discrete models, such as the discrete-element model [1–3], the lattice model [4–8], and the rigid-body-spring model [9–11], as analysis tools for simulating discontinuous deformation. These approaches allow the simulation of crack propagation and its interactions with the coarse aggregates in concrete because they enable the easy modeling of discontinuous deformation. Although the lattice or discrete modeling fits the simulation of complicated fracture behavior, such as that of concrete, the principal drawback of the abovementioned models is that the numerical result is strongly dependent on the mesh pattern and mesh size.

The FEM is a reasonable choice as a tool for structural analysis. Many studies have reported the analysis of the concrete's meso-structure using the FEM, and have achieved the generation of finite element meshes along the geometry of coarse aggregates by replacing the actual aggregates with simple artificial figures such as two-dimensional (2D) circles or polygons in [12–15], and three-dimensional (3D) spheres or polyhedrons in [16–21]. To simulate the fracture behavior of the meso-structure of actual concrete, the problem of mesh generation must first be solved.

Image-based analyses have been conducted using the computed tomography image of concrete to analyze actual concrete's meso-structures [22–26]. Most of these analyses use the Voxel-type FEM, which allows the direct transformation of the digital image into a finite element mesh [27–30]. Although the Voxel FEM has the advantage of easily reflecting the complicated geometry of aggregates using a grid mesh instead of mesh generation in accordance with the geometry, the zigzag-patterned mesh reduces the accuracy of stress at the material interface. Additionally, the requirement of a fine mesh to express a smooth geometry increases the computational cost. In recent years, the virtual element method [31] has been applied to analyze concrete's mesostructures reconstructed by X-ray and neutron-computed tomography images [32]. Computational techniques for modeling the random distribution of coarse aggregates with a complex geometry have also been investigated [33–35].

As an alternative approach for avoiding the difficulty of mesh generation, meshfree or meshless analyses such as the extended FEM (XFEM) [36], the finite cover method (FCM) [37], and other related methods, have been applied to the analysis of heterogeneous solids such as concrete. These methods can analyze the crack growth and the heterogeneous solids without mesh generation along the physical boundaries [38,39]. Moreover, meshless analysis is a possible approach toward simulating the crack growth in the concrete's meso-structure, but its application to the analysis of multiple cracks in heterogeneous solids is difficult, owing to physical boundaries such as cracks or interfaces, which must be captured and traced during the finite element analysis, instead of meshing or re-meshing along the physical boundaries.

The authors have previously investigated a damage model based on the fracture mechanics of concrete [40,41]. By analyzing this model using the FEM, it is possible to simulate the fracture behavior of quasi-brittle materials. The arbitrary crack growth can be expressed using a fine mesh, owing to the method's low dependence on mesh size. The application of

this method to the crack propagation analysis of the mortar phase enables the simulation of the fracture behavior of the concrete's meso-structure, but simulation has not yet been achieved owing to the difficulty of mesh generation, as reported by other studies. Thus, the first point to be addressed is the development of an approach for simulating the fracture behavior of heterogeneous solids in a meshless manner.

This paper proposes a new damage model for simulating the cohesive fracture behavior of multi-phase composite materials such as concrete. A remarkable characteristic of the proposed model is that the formulation is based on the theoretical solution of a one-dimensional (1D) elastic bar problem, which allows the damage evaluation of the matrix phase in multi-phase composite materials using the volume fraction of each material phase. This means that finite element analysis can be carried out without mesh generation along the material interfaces. In other words, the proposed damage model allows a type of meshless analysis using a finite element mesh generated irrespectively of the physical geometries, and is effective in simulating the fracture behavior of the concrete's meso-structure. It is well known that the fracture of concrete is affected by the presence of the interface between the mortar and aggregates. The best thing to simulate the fracture behavior of composite materials like concrete is to model the three-phase structure composed of the matrix, inclusions, and interfaces. This paper, however, focuses on modeling two-phase structures composed of the matrix and inclusions as a first step to simulate the fracture behavior of real concrete.

This paper is organized as follows. Section 2 begins with the formulation of the damage model as a 1D problem, which is then extended to 2D and 3D problems using the equivalent strain and stress. Additionally, the potential of meshless finite element analysis for composite materials is explained. In Section 3, numerical examples are solved for 1D and 2D two-phase composites to verify the validity of the proposed damage model, and the results are compared with reference solutions. Subsequently, the proposed model is applied to the simulation of 3D cohesive crack growth in a heterogeneous solid with a large number of spherical inclusions as an alternative to the concrete's meso-structure. The final section presents the concluding remarks and makes recommendations for future work.

Formulation of damage model

This section presents the formulation of the proposed damage model for simulating the cohesive fracture behavior of multi-phase composite materials. First, the damage model is formulated as a 1D problem based on the elastic solution of a composite bar problem. Then, the 1D formulation is extended to multi-dimensional problems using the equivalent strain and stress. The characteristics of meshless finite element analysis for multi-phase composite materials using the damage model is also described.

Formulation in 1D problems

The tension problem of the two-phase composite bar shown in Fig. 1 is set to formulate the damage model, wherein the composite bar does not include the interface. This section targets the composite bar in which different materials are arranged in series under tensile load to model the tensile damage of multi-phase composite materials. In many cases of multi-phase composites, the stress redistribution due to fracture damages the only

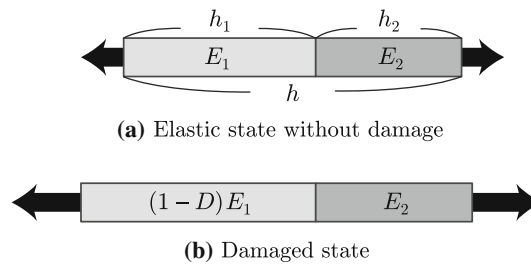


Fig. 1 Tensile problem of an elastic bar comprising two materials: **a** elastic state without damage; **b** damaged state

weakest material. Thus, the damage is assumed to be induced only in Material 1. Let h_1 and E_1 be the length and Young's modulus of Material 1, respectively, and h_2 and E_2 be the length and Young's modulus of Material 2, respectively. The cross-sectional area is constant throughout the bar.

By letting $h = h_1 + h_2$ be the total length of the bar, the volume fraction of Materials 1 and 2 can be expressed as follows:

$$V = \frac{h_1}{h}; \quad 1 - V = \frac{h_2}{h} \quad (1)$$

where V is the volume fraction of Material 1.

First, let us consider the elastic state without damage, as shown in Fig. 1 a. The axial force is constant in the composite bar, wherein different materials are arranged in series. With a constant cross-section, the stress is also constant throughout the bar and can be expressed as follows:

$$\sigma = E_1 \varepsilon_1 = E_2 \varepsilon_2 \quad (2)$$

where ε_1 and ε_2 are the strain of Materials 1 and 2, respectively. From the relationship between the displacement and strain, the average strain of the entire bar can be calculated using the volume fraction of the materials in Eq. (1), as follows:

$$\varepsilon = \frac{\varepsilon_1 h_1 + \varepsilon_2 h_2}{h} = V \varepsilon_1 + (1 - V) \varepsilon_2 \quad (3)$$

Substituting Eq. (2) into Eq. (3) yields the following relationship between the stress and strain of the entire bar:

$$\sigma = \left(\frac{V}{E_1} + \frac{1 - V}{E_2} \right)^{-1} \varepsilon = E \varepsilon \quad (4)$$

where E is the average Young's modulus for the composite bar, and is expressed as follows:

$$E = \left(\frac{V}{E_1} + \frac{1 - V}{E_2} \right)^{-1} \quad (5)$$

Let $\bar{\varepsilon}_1$ be the damage initiation strain of Material 1, and let $\bar{\varepsilon}$ denote the average strain of the composite bar when the strain of Material 1 reaches the damage initiation strain; that is, $\varepsilon_1 = \bar{\varepsilon}_1$. The combination of Eqs. (2) and (3) yields the following relationship between $\bar{\varepsilon}$ and $\bar{\varepsilon}_1$:

$$\bar{\varepsilon} = V \bar{\varepsilon}_1 + (1 - V) \varepsilon_2 = \left\{ V + (1 - V) \frac{E_1}{E_2} \right\} \bar{\varepsilon}_1 = \alpha_0 \bar{\varepsilon}_1 \quad (6)$$

where α_0 is expressed as follows:

$$\alpha_0 = \left\{ V + (1 - V) \frac{E_1}{E_2} \right\} \quad (7)$$

By combining Eqs. (5) and (7), we can also obtain the following relationship between E and E_1 :

$$E = \alpha_0^{-1} E_1 \quad (8)$$

Next, we consider the case wherein Material 1 is in a damaged state, as shown in Fig. 1 b. Let D be the damage variable representing the degree of stiffness degradation, which takes $0 \leq D \leq 1$. Because the axial force is constant throughout the composite bar even when Material 1 is in a damaged state, the stress of the composite bar is expressed as follows:

$$\sigma = (1 - D)E_1\varepsilon_1 = E_2\varepsilon_2 \quad (9)$$

The combination of Eqs. (3) and (9) yields the following relationship between ε and ε_1 , when Material 1 is in a damaged state:

$$\varepsilon = V\varepsilon_1 + (1 - V)\varepsilon_2 = \left\{ V + (1 - V)(1 - D) \frac{E_1}{E_2} \right\} \varepsilon_1 = \alpha_D \varepsilon_1 \quad (10)$$

where α_D is given by the following relationship:

$$\alpha_D = \left\{ V + (1 - V)(1 - D) \frac{E_1}{E_2} \right\} \quad (11)$$

To model the cohesive fracture process in quasi-brittle materials, a fracture mechanics model based on the energy balance approach in terms of fracture energy, as proposed by Hillerborg et al. [42], is introduced into the damage model. Specifically, the following relationship between the cohesive-traction force and the crack-opening displacement on the crack faces, which has the same form as in [43] and as shown in Fig. 2, is used as the fracture mechanics model, as follows::

$$t_1 = \bar{t}_1 \exp \left(-\frac{\bar{t}_1}{G_f} w_1 \right) \quad (12)$$

where t_1 is the cohesive-traction force per unit area, w_1 is the crack-opening displacement, \bar{t}_1 is the fracture (damage) initiation stress, G_f is the fracture energy, and subscript 1 indicates Material 1. Again, note that fracture (damage) initiation is allowed only in Material 1. For 1D problems, the cohesive-traction force accommodates the stress as follows:

$$t_1 = \sigma_1 ; \quad \bar{t}_1 = \bar{\sigma}_1 = E_1 \bar{\varepsilon}_1 \quad (13)$$

where σ_1 and $\bar{\sigma}_1$ are the stress and the fracture (damage) initiation stress of Material 1, respectively. From the relationship between displacement and strain, the crack-opening displacement of Material 1, w_1 can be calculated as follows:

$$w_1 = \varepsilon_1 h_1 - \bar{\varepsilon}_1 h_1 = (\varepsilon_1 - \bar{\varepsilon}_1) h_1 \quad (14)$$

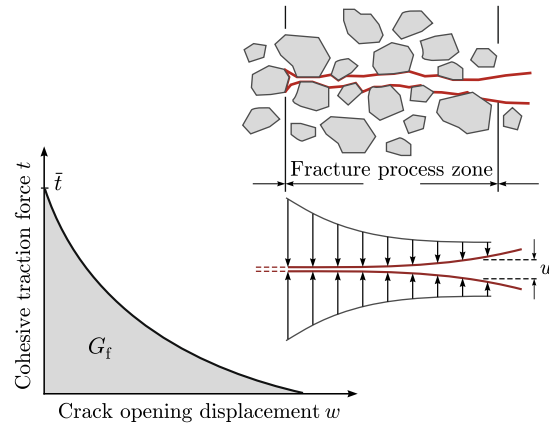


Fig. 2 Relationship between cohesive-traction force and crack-opening displacement in fracture process zone of quasi-brittle materials

The substitution of Eqs. (13) and (14) into (12) yields the following relationship between the stress and strain of Material 1:

$$\sigma_1 = E_1 \bar{\varepsilon}_1 \exp \left\{ -\frac{E_1 \bar{\varepsilon}_1}{G_f} (\varepsilon_1 - \bar{\varepsilon}_1) h_1 \right\} \quad (15)$$

By rearranging Eq. (15) such that it follows the constitutive equation using the damage variable, we obtain the following relationship:

$$\begin{aligned} \sigma_1 &= \frac{\bar{\varepsilon}_1}{\varepsilon_1} \exp \left\{ -\frac{E_1 \bar{\varepsilon}_1}{G_f} (\varepsilon_1 - \bar{\varepsilon}_1) h_1 \right\} E_1 \varepsilon_1 \\ &= \left(1 - \left[1 - \frac{\bar{\varepsilon}_1}{\varepsilon_1} \exp \left\{ -\frac{E_1 \bar{\varepsilon}_1}{G_f} (\varepsilon_1 - \bar{\varepsilon}_1) h_1 \right\} \right] \right) E_1 \varepsilon_1 \\ &= (1 - D) E_1 \varepsilon_1 \end{aligned} \quad (16)$$

where the damage variable D is expressed as follows:

$$D = 1 - \frac{\bar{\varepsilon}_1}{\varepsilon_1} \exp \left\{ -\frac{E_1 \bar{\varepsilon}_1}{G_f} (\varepsilon_1 - \bar{\varepsilon}_1) h_1 \right\} \quad (17)$$

Next, we must derive the constitutive equation for the composite bar involving the damage of Material 1, instead of deriving it only for Material 1. The composite bar wherein different materials are arranged in series with the same cross-section exerts constant stress; that is, $\sigma_1 = \sigma$. Additionally, by substituting Eqs. (1), (6) and (8) into Eq. (16), we can obtain the following constitutive relationship between the stress and strain of the entire bar:

$$\begin{aligned} \sigma &= E \bar{\varepsilon} \exp \left\{ -\frac{E \bar{\varepsilon}}{G_f} \left(\frac{\varepsilon}{\alpha_D} - \frac{\bar{\varepsilon}}{\alpha_0} \right) V h \right\} \\ &= \left(1 - \left[1 - \frac{\bar{\varepsilon}}{\varepsilon} \exp \left\{ -\frac{E \bar{\varepsilon}}{G_f} \left(\frac{\varepsilon}{\alpha_D} - \frac{\bar{\varepsilon}}{\alpha_0} \right) V h \right\} \right] \right) E \varepsilon \\ &= (1 - D) E \varepsilon \end{aligned} \quad (18)$$

where the damage variable D is expressed as follows:

$$D = 1 - \frac{\bar{\varepsilon}}{\varepsilon} \exp \left\{ -\frac{E \bar{\varepsilon}}{G_f} \left(\frac{\varepsilon}{\alpha_D} - \frac{\bar{\varepsilon}}{\alpha_0} \right) V h \right\} \quad (19)$$

Extension to multi-dimensional problems

In multi-dimensional problems, the two-phase 1D composite bar is translated into two-phase composite materials. The constitutive equation for the damage of two-phase composite materials in multi-dimensional problems is expressed as follows:

$$\boldsymbol{\sigma} = (1 - D_e)\mathbf{c} : \boldsymbol{\varepsilon} \quad (20)$$

where $\boldsymbol{\sigma}$ is the Cauchy stress tensor, $\boldsymbol{\varepsilon}$ is the small strain tensor, \mathbf{c} is the elastic coefficient tensor, and D_e is the damage variable in multi-dimensional problems.

Moreover, in multi-dimensional problems, the stress and strain tensors are converted into the equivalent stress and strain to accommodate the unidirectional stress and strain. Specifically, we use the following modified von-Mises criterion [44] as the equivalent strain ε_e because it is suitable to quasi-brittle materials such as concrete:

$$\varepsilon_e = \frac{k-1}{2k(1-2\nu)}I'_1 + \frac{1}{2k}\sqrt{\left(\frac{k-1}{1-2\nu}I'_1\right)^2 + \frac{12k}{(1+\nu)^2}J'_2} \quad (21)$$

where ν is the Poisson's ratio, k is the ratio of tensile to compressive strength, and I'_1 and J'_2 are the first invariant of the strain tensor and second invariant of the deviatoric strain tensor, respectively, and are defined as follows:

$$I'_1 = \text{tr } \boldsymbol{\varepsilon} = \varepsilon_{kk} \quad (22)$$

$$J'_2 = \frac{1}{2}\mathbf{e} : \mathbf{e} = \frac{1}{2}e_{kl}e_{kl}; \quad \mathbf{e} = \boldsymbol{\varepsilon} - \frac{1}{3}\text{tr } \boldsymbol{\varepsilon} \quad (23)$$

Figure 3 shows the contour plots of the equivalent strain based on the modified von-Mises criterion in the principal strain space for different values of the strength ratio, k . As can be seen in the plots, the equivalent strain is capable of representing a compressive strength higher than the tensile strength, which is essential for modeling the fracture of quasi-brittle materials.

Let σ_e be the equivalent stress obtained from the equivalent strain, that is, ε_e . Because the equivalent stress and strain are scalar values corresponding to unidirectional problems, they can be related using 1D constitutive equations. This implies that the above-mentioned formulation for 1D problems can be applied. Accordingly, the relationship between the equivalent stress and strain corresponding to the constitutive equation in multi-dimensional problems can be expressed as follows:

$$\begin{aligned} \sigma_e &= E\bar{\varepsilon}_e \exp \left\{ -\frac{E\bar{\varepsilon}_e}{G_f} \left(\frac{\varepsilon_e}{\alpha_D} - \frac{\bar{\varepsilon}_e}{\alpha_0} \right) Vh_e \right\} \\ &= \left(1 - \left[1 - \frac{\bar{\varepsilon}_e}{\varepsilon_e} \exp \left\{ -\frac{E\bar{\varepsilon}_e}{G_f} \left(\frac{\varepsilon_e}{\alpha_D} - \frac{\bar{\varepsilon}_e}{\alpha_0} \right) Vh_e \right\} \right] \right) E\varepsilon_e \\ &= (1 - D_e)E\varepsilon_e \end{aligned} \quad (24)$$

where $\bar{\varepsilon}_e$ is the fracture (damage) initiation strain in multi-dimensional problems, h_e is the length of the multi-dimensional domain, which can also be considered as the representative length of the element whose damage is evaluated, and D_e is the damage variable in multi-dimensional problems and expressed as follows:

$$D_e = 1 - \frac{\bar{\varepsilon}_e}{\varepsilon_e} \exp \left\{ -\frac{E\bar{\varepsilon}_e}{G_f} \left(\frac{\varepsilon_e}{\alpha_D} - \frac{\bar{\varepsilon}_e}{\alpha_0} \right) Vh_e \right\} \quad (25)$$

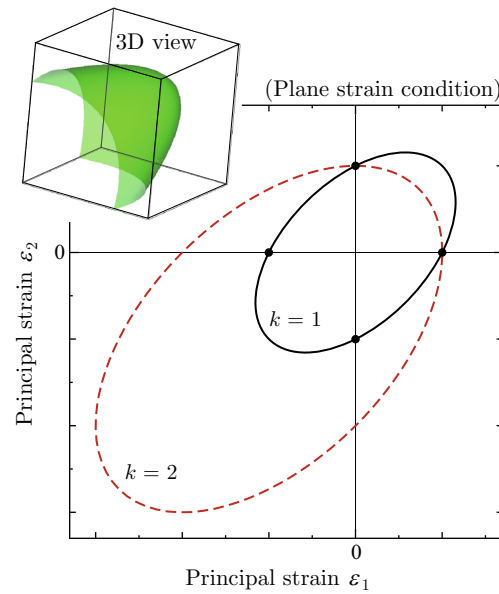


Fig. 3 Contour plot of modified von-Mises criterion

The abovementioned formulation results in the damage model of two-phase materials. Naturally, the damage model is also applicable to multi-phase composite materials.

Governing equation for quasi-static equilibrium

The damage variable D_e given in Eqs. (24) and (25) allows the damage evaluation of multi-phase composite materials. Thus, the governing equations for the quasi-static equilibrium of an elastic continuum involving damage are expressed as follows:

$$\nabla \cdot \boldsymbol{\sigma} + \bar{\mathbf{b}} = \mathbf{0} \quad \text{in } \Omega \quad (26)$$

$$\boldsymbol{\varepsilon} = \frac{1}{2} \left\{ \nabla \mathbf{u} + (\nabla \mathbf{u})^T \right\} \quad \text{in } \Omega \quad (27)$$

$$\boldsymbol{\sigma} = (1 - D_e) \mathbf{c} : \boldsymbol{\varepsilon} \quad \text{in } \Omega \quad (28)$$

where $\bar{\mathbf{b}}$ is the given body force vector, \mathbf{u} is the displacement vector, Ω is the entire domain, and ∇ is the nabla operator for calculating the gradients.

Application to finite element analysis

As can be seen in Eq. (28) from the governing equations, the proposed damage model can be subjected to finite element analysis simply by introducing the damage variable (easily calculated using the equivalent strain) into Hooke's law.

To calculate the damage variable, the length of the multi-dimensional domain h_e shown in Eq. (24) must be determined. Here, h_e conforms to the total length h of the composite bar in 1D problems, as shown in Fig. 1, and corresponds to the length of the finite element in 1D finite element analysis. In 2D or 3D finite element analysis, h_e accommodates the representative length of finite elements, as shown schematically in Fig. 4. In the numerical examples presented in Section 3, unstructured random meshes were prepared with triangular elements for 2D problems and with tetrahedral elements for 3D problems so as to reduce the dependency of mesh configuration on the damage (crack) propagation

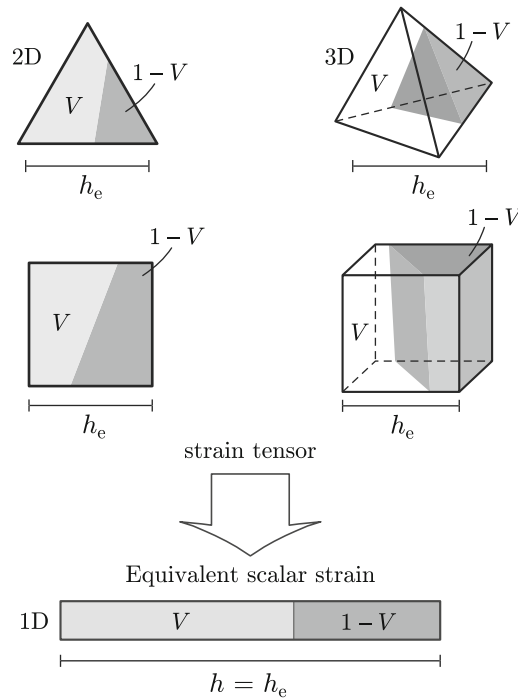


Fig. 4 Conversion of multi-dimensional problems into 1D problems

behavior. In this study, the representative length of the finite elements was estimated as follows:

$$h_e = \sqrt{2A_e} \quad \text{for 2D triangular finite elements} \quad (29)$$

$$h_e = (12V_e)^{1/3} \quad \text{for 3D tetrahedral finite elements} \quad (30)$$

where A_e is the area of the 2D finite element and V_e is the volume of the 3D finite element. The multiplier of 2 in Eq. (29) for the triangular elements results from the assumption whereby two triangles form a quadrilateral. Similarly, the multiplier of 12 in Eq. (30) for the tetrahedral elements is based on the assumption whereby 12 tetrahedrons form a hexahedron.

Capability for meshless finite element analysis

The proposed damage model is based on the theoretical solution of 1D elastic composite bar problems, and allows the damage evaluation of the matrix-phase in composite materials using the volume fraction of the matrix. An important point is that the presence of each material-phase can be expressed only by the volume ratio, and does not require the physical shape.

In multi-dimensional problems, the multi-axial strain fields are replaced by a uni-axial bar problem using the equivalent strain, as shown in Fig. 4. Thus, it becomes possible to evaluate the damage of the matrix-phase in composite materials using only the volume ratio, in the same manner as for multi-dimensional problems. This implies that, in the finite element analysis, the mesh configuration does not need to conform to the physical boundaries of composite materials. In other words, the finite element mesh can be gen-

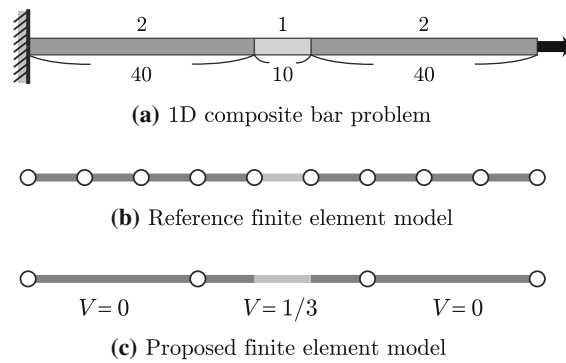


Fig. 5 Tensile problem of bar comprising two different materials

erated irrespectively of the physical boundaries, which enables a type of meshless finite element analysis.

Verification of damage model

The proposed damage model enables the damage evaluation of the matrix-phase in composite materials within the framework of meshless finite element analysis. This section presents several numerical examples to verify the validity of the damage model and demonstrate the availability of meshless finite element analysis.

Verification example in 1D

First, the verification of the proposed damage model is carried out for 1D problems. The analysis target is a composite bar composed of two different materials subjected to a tensile load, as shown in Fig. 5 a. Only Material 1 in the center of the bar is assumed to be damaged. The material parameters are as follows: $E_1 = 20$ GPa, $\bar{\varepsilon}_1 = 0.0002$, $G_f = 0.05$ N/mm, $E_2 = 60$ GPa.

Figure 5 b shows the finite element mesh for the reference solution, wherein the composite bar is divided into nine elements according with the material configuration at equal intervals. Reference analysis was performed by applying the original damage model [40] to Material 1 in the reference finite element mesh. Figure 5 c shows the finite element mesh for the proposed damage model. In the proposed model, the mesh generation conforming to the material interfaces is not required; therefore, it suffices to prepare three elements irrespectively of the material configuration, and provide each element with the volume fraction of Material 1.

Figure 6 compares the load–displacement responses obtained by the reference analysis and the proposed analysis. The horizontal axis indicates the apparent strain calculated as the displacement divided by the length of the model, while the vertical axis represents the apparent stress defined as the load divided by the loading area. The results confirmed that the proposed model has good fit to the reference solution and allows the damage evaluation of Material 1 within the element by only using the volume fraction. This indicates the validity of the damage model based on the elastic solution of a 1D composite bar problem.

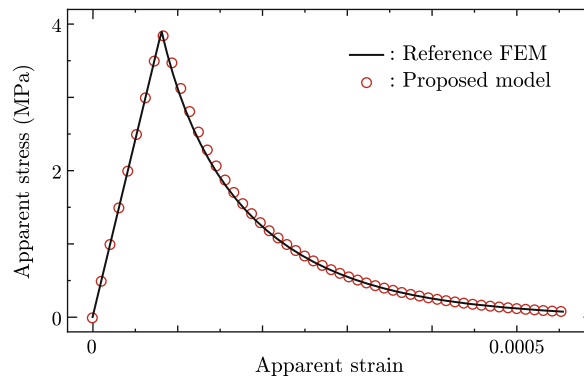


Fig. 6 Comparison of load–displacement curves in 1D bar problem

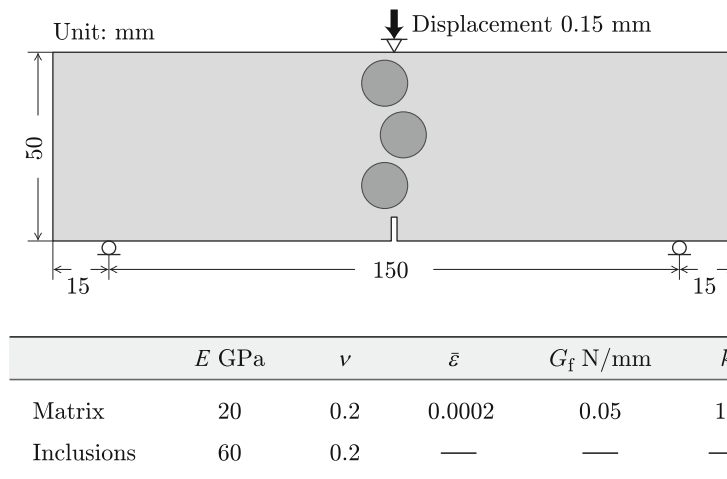


Fig. 7 Three-point bending problem of beam with three circular inclusions

Verification example in 2D

Next, the validity of the proposed damage model was verified for 2D problems. Unlike 1D problems, the damage may be evaluated by using the equivalent strain. The main difference from 1D problems is that the equivalent strain is used in finite element analysis with the damage model.

The analysis target is a beam with a single-edge notch subjected to three-point bending under the plane strain condition, as shown in Fig. 7. To investigate the crack propagation behavior, the beam has three circular inclusions in the region where the crack propagates. The material parameters of the matrix and the inclusions are presented in Fig. 7, and it is assumed that the inclusions do not fracture.

Figure 8 shows two finite element mesh types. The mesh sizes are determined such that the inclusion geometries can be sufficiently reproduced. The finite element mesh in Fig. 8a was generated according to the material interfaces, and used for reference analysis. Figure 8b presents the finite element mesh for applying the proposed damage model; the mesh was generated irrespectively of the material interfaces. The difference of the meshes is obvious, as can be seen from the enlarged view shown in Figure 8 (c).

Figure 9 compares the load–displacement curves obtained from the reference analysis and proposed analysis. The response obtained from the proposed model is in good agree-

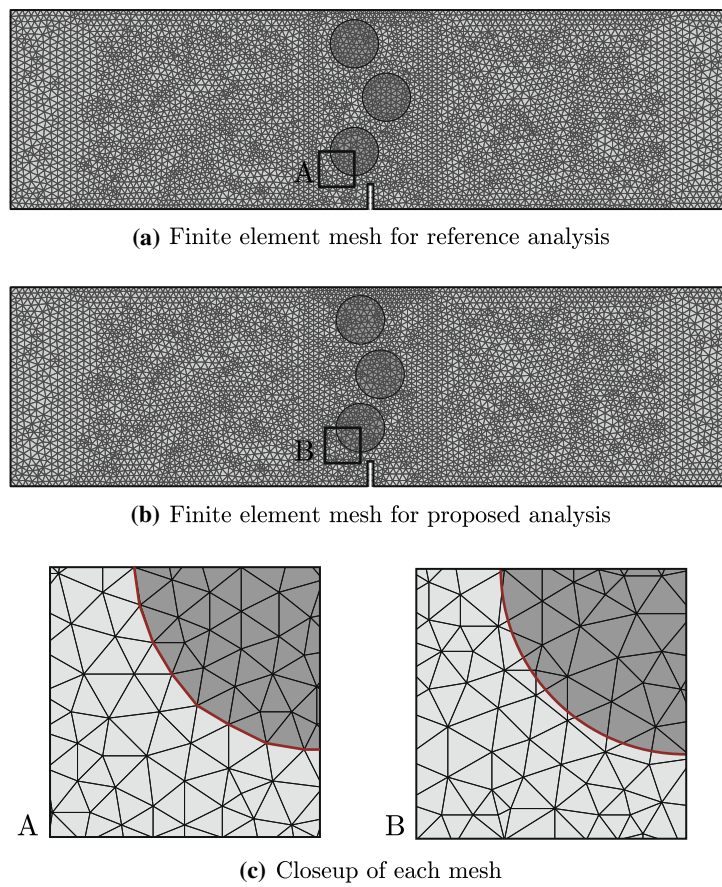


Fig. 8 Finite element meshes for 2D three-point bending problem

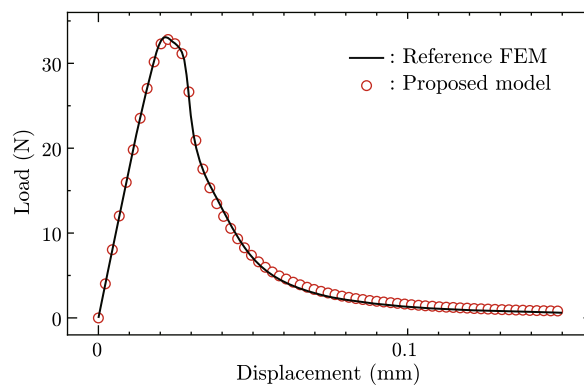


Fig. 9 Comparison of load-displacement curves in 2D beam problem

ment with the reference solution. This means that, in the same manner as for 2D problems, the proposed damage model is capable of evaluating the damage of the matrix-phase in composite materials using the volume fraction of the matrix within the element.

The distributions of equivalent strain are shown in Fig. 10. The damage in the proposed model is evaluated based on the equivalent strain, and the strain localization in such an analysis with a damage model can be considered as cracking. Thus, it becomes possible to visualize the crack propagation behavior by displaying the equivalent strain distribution,

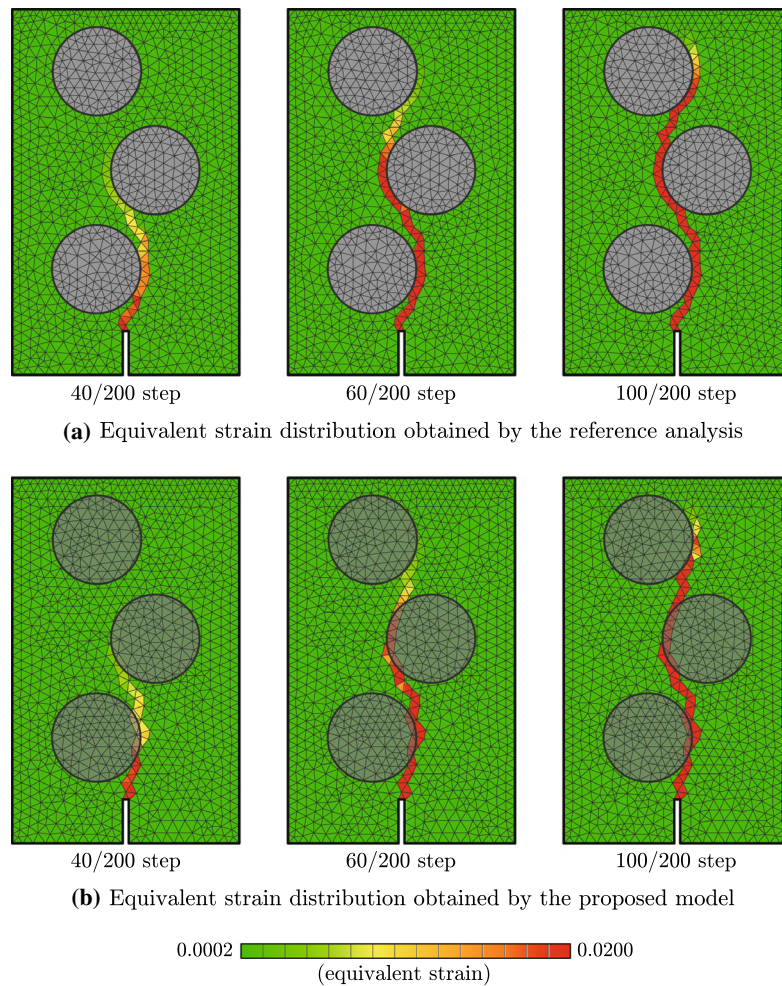


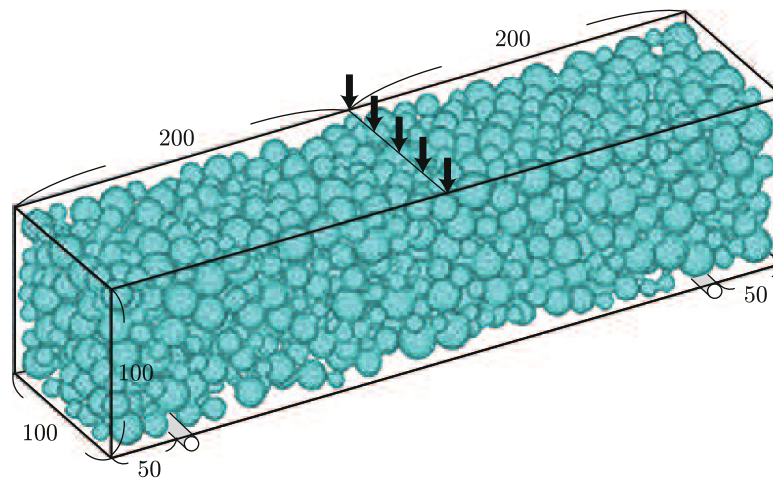
Fig. 10 Comparison of damage propagation: left figures show the reference solutions; right figures present the results obtained by the proposed model

which takes the damage initiation strain as the minimum value, as shown in Fig. 10. For convenience, the strain localization caused by damage is referred to as “crack” in this paper.

The comparison of these results revealed that the path and rate of crack propagation are approximately the same, and thus the proposed model is capable of evaluating only the matrix-phase damage within elements arranged irrespectively of the material interfaces. The damage model formulated in this paper can also obtain satisfactory results for 2D problems.

Application to 3D problem

Finally, the availability and applicability of the proposed model is demonstrated for a 3D problem, for which it is very difficult to prepare a finite element mesh. The analysis target is a concrete-like beam subjected to three-point bending. The concrete includes a large number of coarse aggregates, as shown in Figure 11. For simplicity, the aggregates are considered as spherical inclusions with different sizes, and each of them is arranged as densely as possible within the beam.



	E GPa	ν	$\bar{\varepsilon}$	G_f N/mm	k
Matrix	20	0.2	0.0002	0.05	10
Inclusions	60	0.2	—	—	—

Fig. 11 Three-point bending problem for beam with many spherical inclusions

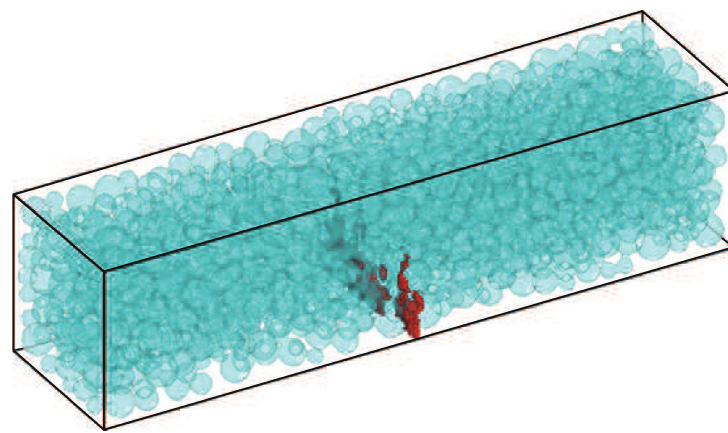
The finite element mesh is prepared irrespective of the spherical aggregate geometries. A random mesh with tetrahedral elements is used because it has good compatibility for reducing the mesh dependency on the damage propagation behavior. The total number of finite elements and nodes is approximately 4.4 million and 0.8 million, respectively. The material properties of the matrix and inclusions are presented in Fig. 11. Because it is impractical to generate a finite element mesh in accordance with the physical geometries, only numerical analysis was conducted for the proposed model.

The distribution of equivalent strain is shown in Fig. 12, along with an enlarged view of the center of the beam. The result shows the cracks propagating around the spherical coarse aggregates, which is similar to the cracking of actual concrete and confirms that the proposed model allows crack propagation analysis for such an extremely complicated 3D problem. Additionally, it can be seen that the meshless analysis of heterogeneous solids can also be performed without mesh generation according to the physical geometries, which implies that the proposed damage model can successfully simulate the cohesive fracture behavior of the meso-structure of actual concrete.

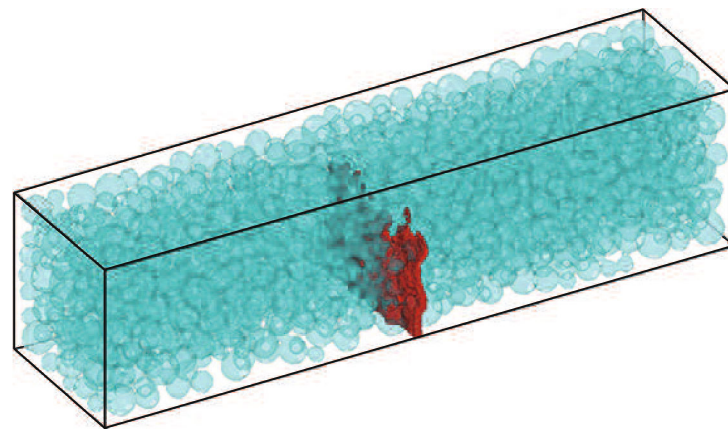
Conclusion

This paper presented a new damage model for simulating the cohesive fracture behavior of multi-phase composite materials. An outstanding feature of the proposed model is its capability of evaluating the matrix-phase damage within an element comprising different materials, which thus enables the meshless finite element analysis of crack growth in composite materials. This is attributed to the formulation of the damage model on the basis of a theoretical solution of 1D elastic composite bar problems.

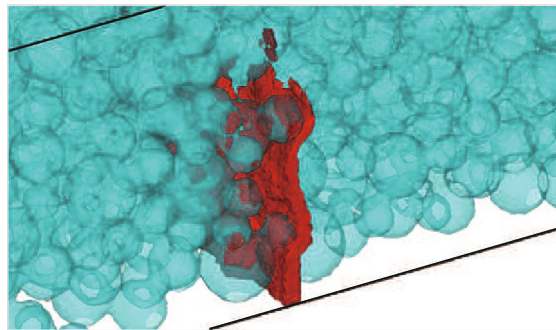
Several numerical examples were presented to demonstrate the validity and availability of the proposed model. The validity of the formulation based on the elastic solution of



(a) Crack propagation at 90/300 step



(b) Crack propagation at 130/300 step



(c) Closeup at 130/300 step

Fig. 12 Distribution of damage: 3D crack propagation behavior in highly heterogeneous solid

composite bar problems was first verified for a 1D problem. Then, a 2D problem was solved to verify the capability of evaluating the damage of the matrix-phase in composite materials. The numerical result also revealed that the proposed model allows the meshless finite element analysis of crack propagation behavior in multi-phase composite materials using the volume fraction of the matrix within the element, instead of generating a finite element mesh in accordance with the material interfaces. Finally, the proposed model was applied to the simulation of 3D cohesive crack growth in a heterogeneous solid with a large number of spherical inclusions, and the obtained results demonstrated that the

proposed damage model can potentially simulate the cohesive fracture behavior of the meso-structure of actual concrete.

For simplicity, our results are limited to the analysis of two-phase heterogeneous materials with circular or spherical inclusions without interfaces. However, owing to its meshless nature, the proposed model is also applicable to the analysis of real composite materials with arbitrarily-shaped inclusions, such as concrete. To this end, future work should formulate the interfacial damage between the matrix and inclusions and demonstrate that the damage model facilitates the analysis of cohesive crack growth in the micro- or meso-structure of actual composite materials. Besides, the damage model should also be examined for its applicability to fracture problems subjected to other loading patterns.

Acknowledgements

Not applicable.

Author contributions

MK: Writing, Review, Code implementation, Code verification. TK: Verification analysis, Application to 3D problem. HS: Verification analysis, Application to 3D problem. All authors read and approved the final manuscript.

Funding

This study was supported by JSPS KAKENHI (Grant Numbers 16H02137 and 16K17549), whose support we gratefully acknowledge.

Availability of data and materials

Not applicable.

Declarations

Competing interests

The authors declare that they have no competing interests.

Received: 11 August 2022 Accepted: 10 December 2022

Published online: 06 February 2023

References

1. Azevedo NM, Lemos JV, de Almeida JR. Influence of aggregate deformation and contact behaviour on discrete particle modelling of fracture of concrete. *Eng Fract Mech.* 2008;75:1569–86.
2. Nitka M, Tejchman J. A three-dimensional meso-scale approach to concrete fracture based on combined DEM with X-ray μ CT images. *Cem Concr Res.* 2018;107:11–29.
3. Rangari S, Murali K, Deb A. Effect of meso-structure on strength and size effect in concrete under compression. *Comput Struct.* 2018;195:162–85.
4. Prado EP, van Mier JGM. Effect of particle structure on mode I fracture process in concrete. *Eng Fract Mech.* 2003;70:1793–803.
5. Leite JPB, Slowik V, Mihashi H. Computer simulation of fracture processes of concrete using mesolevel models of lattice structures. *Cem Concr Res.* 2004;34:1025–33.
6. Grassl P, Jirasek M. Meso-scale approach to modelling the fracture process zone of concrete subjected to uniaxial tension. *Int J Solids Struct.* 2010;47:957–68.
7. Asahina D, Landis EN, Bolander JE. Modeling of phase interfaces during pre-critical crack growth in concrete. *Cem Concr Compos.* 2011;33:966–77.
8. Lale E, Rezakhani R, Alnaggar M, Cusatis G. Homogenization coarse graining (HCG) of the lattice discrete particle model (LDPM) for the analysis of reinforced concrete structures. *Eng Fract Mech.* 2018;197:259–77.
9. Bolander JE Jr, Saito S. Fracture analyses using spring networks with random geometry. *Eng Fract Mech.* 1998;61:569–91.
10. Nagai K, Sato Y, Ueda T. Mesoscopic Simulation of Failure of Mortar and Concrete by 3D RBSM. *J Adv Conc Tech.* 2005;3:385–402.
11. Gedik YH, Nakamura H, Yamamoto Y, Kunieda M. Evaluation of three-dimensional effects in short deep beams using a rigid-body-spring-model. *Cem Concr Compos.* 2011;33:978–91.
12. Tjssens MGA, Sluys LJ, van der Giessen E. Simulation of fracture of cementitious composites with explicit modeling of microstructural features. *Eng Fract Mech.* 2001;68:1245–63.
13. Zhou XQ, Hao H. Modelling of compressive behaviour of concrete-like materials at high strain rate. *Int J Solids Struct.* 2008;45:4648–61.
14. Du X, Jin L, Ma G. Numerical simulation of dynamic tensile-failure of concrete at meso-scale. *Int J Impact Eng.* 2014;66:5–17.
15. Wang XF, Yang ZJ, Yates JR, Jivkov AP, Zhang Ch. Monte Carlo simulations of mesoscale fracture modelling of concrete with random aggregates and pores. *Constr Build Mater.* 2015;75:35–45.

16. Caballero A, Lopez CM, Carol I. 3D meso-structural analysis of concrete specimens under uniaxial tension. *Comput Methods Appl Mech Eng*. 2006;195:7182–95.
17. Hafner S, Eckardt S, Luther T, Konke C. Mesoscale modeling of concrete: Geometry and numerics. *Comput Struct*. 2006;84:450–61.
18. Kim S-M, Al-Rub RKA. Meso-scale computational modeling of the plastic-damage response of cementitious composites. *Cem Concr Res*. 2011;41:339–58.
19. Wang X, Zhang M, Jivkov AP. Computational technology for analysis of 3D meso-structure effects on damage and failure of concrete. *Int J Solids Struct*. 2016;80:310–33.
20. Yilmaz O, Molinari J-F. A mesoscale fracture model for concrete. *Cem Concr Res*. 2017;97:84–94.
21. Shen L, Ren Q, Zhang L, Han Y, Cusatis G. Experimental and numerical study of effective thermal conductivity of cracked concrete. *Constr Build Mater*. 2017;153:55–68.
22. Ren W, Yang Z, Sharma R, Zhang Ch, Withers PJ. Two-dimensional X-ray CT image based meso-scale fracture modelling of concrete. *Eng Fract Mech*. 2015;133:24–39.
23. Li S, Li Q. Method of meshing ITZ structure in 3D meso-level finite element analysis for concrete. *Finite Elements Anal Des*. 2015;93:96–106.
24. Trawinski W, Teichman J, Bobinski J. A three-dimensional meso-scale modelling of concrete fracture based on cohesive elements and X-ray μ CT images. *Eng Fract Mech*. 2018;189:27–50.
25. Liu T, Qin S, Zou D, Song W, Teng J. Mesoscopic modeling method of concrete based on statistical analysis of CT images. *Constr Build Mater*. 2018;192:429–511.
26. Yang X-J, Li B-B, Wu J-Y. X-ray computed tomography images based phase-field modeling of mesoscopic failure in concrete. *Eng Fract Mech*. 2019;208:151–70.
27. Mishnaevsky LL Jr. Automatic voxel-based generation of 3D microstructural FE models and its application to the damage analysis of composites. *Mater Sci Eng*. 2005;407:11–23.
28. Nagai G, Yamada T. Three-dimensional finite element modeling for concrete materials using digital image and embedded discontinuous element. *Int J Multiscale Comput Eng*. 2006;4:461–74.
29. Huang Y, Yang Z, Ren W, Liu G, Zhang C. 3D meso-scale fracture modelling and validation of concrete based on in-situ X-ray Computed Tomography images using damage plasticity model. *Int J Solids Struct*. 2015;15:340–52.
30. Huang Y, Yan D, Yang Z, Liu G. 2D and 3D homogenization and fracture analysis of concrete based on in-situ X-ray Computed Tomography images and Monte Carlo simulations. *Eng Fract Mech*. 2016;163:37–54.
31. Beirão da Veiga L, Brezzi F, Marini LD. Virtual Elements for Linear Elasticity Problems. *SIAM J Numer Anal*. 2013;51:794–812.
32. Kim HT, Park K. Computed tomography (CT) Image-based analysis of concrete microstructure using virtual element method. *Compos Struct*. 2022;299: 115937.
33. Garboczi EJ. Three-dimensional mathematical analysis of particle shape using X-ray tomography and spherical harmonics: application to aggregates used in concrete. *Cem Concr Res*. 2002;32:1621–38.
34. Zhou R, Song Z, Lu Y. 3D mesoscale finite element modelling of concrete. *Comput Struct*. 2017;192:96–113.
35. Salemi M, Wang H. Image-aided random aggregate packing for computational modeling of asphalt concrete microstructure. *Constr Build Mater*. 2018;177:467–76.
36. Moës N, Dolbow J, Belytschko T. A finite element method for crack growth without remeshing. *Int J Numer Methods Eng*. 1999;46:131–50.
37. Terada K, Asai M, Yamagishi M. Finite cover method for linear and nonlinear analyses of heterogeneous solids. *Int J Numer Meth Eng*. 2003;58:1321–46.
38. Li H, Li J, Yuan H. A review of the extended finite element method on macrocrack and microcrack growth simulations. *Theor Appl Fract Mech*. 2018;97:236–49.
39. Kurumatani M, Terada K. Finite cover method with multi-cover layers for the analysis of evolving discontinuities in heterogeneous media. *Int J Numer Meth Eng*. 2009;79:1–24.
40. Kurumatani M, Terada K, Kato J, Kyoya T, Kashiwayama K. An isotropic damage model based on fracture mechanics for concrete. *Eng Fract Mech*. 2016;155:49–66.
41. Kurumatani M, Soma Y, Terada K. Simulations of cohesive fracture behavior of reinforced concrete by a fracture-mechanics-based damage model. *Eng Fract Mech*. 2019;206:392–407.
42. Hillerborg A, Mod  r M, Petersson PE. Analysis of crack formation and crack growth in concrete by means of fracture mechanics and finite elements. *Cem Concr Res*. 1976;6:773–82.
43. Wells GN, Sluys LJ. Application of embedded discontinuities for softening solids. *Eng Fract Mech*. 2000;65:263–81.
44. de Vree JHP, Brekelmans WAM, van Gils MAJ. Comparison of nonlocal approaches in continuum damage mechanics. *Comput Struct*. 1995;55:581–8.

Publisher's Note

Springer Nature remains neutral with regard to jurisdictional claims in published maps and institutional affiliations.